Development/Plasticity/Repair

Experience-Dependent Switch in Sign and Mechanisms for Plasticity in Layer 4 of Primary Visual Cortex

Lang Wang,[1] Alfredo Fontanini,[1] and Arianna Maffei[1,2]

[1]Department of Neurobiology and Behavior and [2]SUNY Eye Institute, State University of New York–Stony Brook, Stony Brook, New York 11794

Neural circuits are extensively refined by sensory experience during postnatal development. How the maturation of recurrent cortical synapses may contribute to events regulating the postnatal refinement of neocortical microcircuits remains controversial. Here we show that, in the main input layer of rat primary visual cortex, layer 4 (L4), recurrent excitatory synapses are endowed with multiple, developmentally regulated mechanisms for induction and expression of excitatory synaptic plasticity. Maturation of L4 synapses and visual experience lead to a sharp switch in sign and mechanisms for plasticity at recurrent excitatory synapses in L4 at the onset of the critical period for visual cortical plasticity. The state of maturation of excitatory pyramidal neurons allows neurons to engage different mechanisms for plasticity in response to the same induction paradigm. Experience is determinant for the maturation of L4 synapses, as well as for the transition between forms of plasticity and the mechanisms they may engage. These results indicate a tight correlation between the effects of sensory drive and maturation on cortical neurons and provide a new set of cellular mechanisms engaged in the postnatal refinement of cortical circuits.

Introduction

Neural circuits in sensory cortices are sensitive to environmental inputs during specific developmental windows (Hubel and Wiesel, 1970; Hensch, 2004; Tagawa et al., 2005). In rodent primary visual cortex (V1), multiple windows of sensitivity were identified during postnatal development (Feller and Scanziani, 2005; Tagawa et al., 2005; Li et al., 2006; Farley et al., 2007; Tanaka et al., 2009). The best studied window, the critical period (Hubel and Wiesel, 1970), extends from postnatal day 21 (P21) to P28 (Fagiolini et al., 1994). During this epoch, reduction of visual drive is associated with ocular dominance shifts, the rewiring of cortical territories activated by the two eyes (Hubel and Wiesel, 1970; Frenkel and Bear, 2004; Feller and Scanziani, 2005). A second window, the precritical period (Feller and Scanziani, 2005), begins at eye opening and extends to P21. This epoch is associated with intense experience-dependent rewiring (Desai et al., 2002; Majewska and Sur, 2003; Maffei et al., 2004; Wallace and Bear, 2004), without ocular dominance shifts (Fagiolini et al., 1994). The role of experience and maturation in the transition between these periods is hotly debated (McGee et al., 2005; Corlew et al., 2007; Di Cristo et al., 2007; Katagiri et al., 2007; Bélanger and Di Cristo, 2011; Mellios et al., 2011).

Many forms of plasticity contribute to cortical circuit refinement and function during postnatal development (Kirkwood et al., 1996; Desai et al., 2002; Maffei et al., 2006; Crozier et al., 2007; Maffei and Turrigiano, 2008b; Nataraj et al., 2010). Excitatory synapses in particular may be involved differently in experience-dependent refinement depending on the location (Trachtenberg et al., 2000; Desai et al., 2002; Rao and Daw, 2004; Maffei et al., 2006; Crozier et al., 2007; Maffei and Turrigiano, 2008b). Plasticity at excitatory synapses in layer 2/3 (L2/3) and L5 likely contributes to V1 function throughout life (Desai et al., 2002; Wang and Daw, 2003; Jiang et al., 2007; Nataraj et al., 2010), whereas excitatory synapses in L4 seem to have lost their capability for plasticity by P14 (Desai et al., 2002; Wang and Daw, 2003; Daw et al., 2004; Jiang et al., 2007).

Here we report that recurrent excitatory synapses between L4 pyramidal neurons are plastic beyond P14 and that their plasticity depends on the state of maturation of neurons and on visual experience. In the week from P16 to P21, two forms of long-term depression (LTD) are induced by engaging either metabotropic glutamate receptor (mGluR) or NMDA receptor (NMDAR)-dependent mechanisms. After P21, L4 synapses become attuned to one activity paradigm reliably inducing NMDA-dependent long-term potentiation (LTP). Lack of visual drive prevents the shift from LTD to LTP in the critical period. L4 recurrent excitatory synapses may thus engage different cellular mechanisms for induction and expression of long-term synaptic plasticity in different developmental time windows. The developmental regulation of sign and mechanism for synaptic plasticity in L4 indicates that healthy circuit wiring does not depend on a general capability for plasticity but on the recruitment of appropriate mechanisms for plasticity at specific time windows.

Received Feb. 9, 2012; revised June 1, 2012; accepted June 8, 2012.

Author contributions: L.W., A.F., and A.M. designed research; L.W. performed research; L.W. and A.M. analyzed data; L.W., A.F., and A.M. wrote the paper.

This work was supported by National Institutes of Health Grant R01 EY019885 (A.M.) and The Esther A. and Joseph Klingenstein Fund (A.F.). We thank Dr. Yury Garkun, Trevor Griffen, Michelle Kloc, Dr. Lorna Role (State University of New York–Stony Brook, Stony Brook, NY), and Dr. Gina Turrigiano (Brandeis University, Waltham, MA) for useful comments and discussion on data and this manuscript.

Correspondence should be addressed to Arianna Maffei, Department of Neurobiology and Behavior, Life Science Building, Room 546, State University of New York–Stony Brook, Stony Brook, NY 11794. E-mail: arianna.maffei@stonybrook.edu.

DOI:10.1523/JNEUROSCI.0622-12.2012

 0270-6474/12/3210562-12$15.00/0

Materials and Methods

Electrophysiology. Experimental procedures were approved by the Stony Brook University Animal Use Committee and followed the guidelines of the National Institutes of Health. Acute slice preparation and multiple patch-clamp recordings were obtained from rats of both sexes as reported previously (Maffei et al., 2004, 2006). To test for the presence of monosynaptic connections, quadruple simultaneous whole-cell patch-clamp recordings were obtained from visually identified pyramidal neurons in L4 of the monocular region of rat V1. The membrane potential of patched neurons was on average -73 ± 0.7 mV. For uniform comparisons of monosynaptic EPSPs, at the beginning of the recording, a small direct current was injected in the recorded neuron to bring the membrane potential to -70 mV. Neurons diverging >10% from this value during the course of the recording were not included in the analysis. Trains of five action potentials at 20 Hz were elicited in each neuron at different time intervals, and monosynaptic EPSP responses were identified by calculating the spike-triggered average of the membrane potential traces recorded from putative postsynaptic neurons. Once the synaptic response was identified based on its time locking with the corresponding presynaptic action potential (<2 ms delay), a 10 min baseline was recorded to determine the properties of the synaptic response (see data in Fig. 1). After the acquisition of a stable baseline, the protocol for induction of plasticity was applied. For induction protocols, spike timing LTD, presynaptic and postsynaptic neurons were activated above threshold using 5 ms long square pulses of current injection. Both neurons were made to fire 10 action potentials at 20 Hz, and the pairing was repeated 20 times at 0.1 Hz. Three presynaptic and postsynaptic time delays were tested: ± 10 and 0 ms. For slow-wave presynaptic bursting, 10 presynaptic action potentials at 50 Hz were elicited in the presynaptic neuron, whereas the postsynaptic neuron was at -70 mV with the membrane potential free to follow changes attributable to the activation of postsynaptic receptors (see insets in Figs. 4*A* and 5*A*). The interburst frequency was 0.1 Hz, mimicking a slow-wave pattern of activity similar to that reported for neurons in developing visual cortex (Rochefort et al., 2009). For pairing to test the involvement of presynaptic NMDARs, presynaptic bursts of action potentials were the same as those described for slow-wave presynaptic bursting. Each burst was paired with a 300 ms hyperpolarizing step of the postsynaptic neuron to -90 mV. The hyperpolarizing step was started before the burst to allow complete membrane hyperpolarization and avoid potential confounds attributable to presynaptic bursting on the decaying phase of the postsynaptic membrane potential. Synaptic events were monitored for at least 50 min after induction. To quantify the magnitude of plasticity for each pair, the average baseline amplitude was compared with the average EPSP amplitude recorded from 40 to 50 min after induction. Paired *t* tests within pairs were applied to test for significant changes.

Visual deprivation. Monocular deprivation (MD) was obtained by suturing on eye shut (Maffei et al., 2004, 2006, 2010; Maffei and Turrigiano, 2008b) starting at P24 $\pm$ 1 for 4 d. Briefly, animals were anesthetized with a mixture of ketamine (70 mg/kg), xylazine (5 mg/kg), and acepromazine (0.3 mg/kg). Once the animals were deeply anesthetized, the area surrounding one of the eyes was thoroughly cleaned with isopropanol and coated with lidocaine gel to provide local analgesia. The eye was moisturized with eye drops, and four mattress sutures were placed using polyester suture thread (Ethicon 6-0). After the procedure, the animals were allowed to recover on a heating pad and brought back to the animal facility only when fully alert. The eyelid suture and slice preparation were blind to the experimenter.

Post hoc *neuron identification.* After recording, slices were fixed in 4% paraformaldehyde for 1 week. After that, they were washed in PBS, permeabilized with 1% Triton X-100 for 2 h, and then incubated overnight at 4°C in a solution containing streptavidin–Alexa Fluor 488 at 1:2000 in PBS and 0.1% Triton X-100. After a final wash in PBS, slices were mounted with fluoromount and imaged with a fluorescent microscope (Carl Zeiss Axioskop). Only neurons with pyramidal morphology localized in L4 of the monocular portion of V1 were included in the analysis.

Statistical analyses for electrophysiology data. Data are mean $\pm$ SEM. Statistical significance was determined with two-tailed unpaired *t* tests. Paired *t* tests of baseline versus 40–50 min post-induction EPSP verified effective plasticity induction within each recorded pair. Bonferroni's correction was applied for multiple comparisons. To test for differences across conditions, one-way ANOVA were applied and followed by *post hoc* unpaired *t* tests. p values ≤ 0.05 were considered significant.

Quantal analyses. To assess the site of expression of spike timing LTD, slow-wave LTD and slow-wave LTP quantal analysis of EPSP amplitude was performed following the method reported by Sola et al. (2004). Briefly, to make predictions of neurotransmitter mechanisms, we applied a binomial model (Wernig, 1975) in which the probability of release (p) and the number of release sites (n) can be calculated from the average amplitude ($M = mq$, where m is the mean quantum content and q is the quantum size) and the coefficient of variation (CV) of EPSP amplitude ($CV = SD/M$, where SD is standard deviation of EPSP amplitude). In this model, $M = np/q$; $SD^2 = [np \times (1 - p)]$. Application of this binomial model offers a precise interpretation of the inequality: $CVb^2/CVa^2 \Leftrightarrow Mb/Ma$, in which a and b represent two different conditions, in our case baseline (a) and after induction (b), and $\Leftrightarrow$ indicates smaller than, equal, or larger than. This inequality has been used extensively to interpret mechanisms for long-term synaptic plasticity (Bekkers and Stevens, 1990; Malinow and Tsien, 1990). According to this model, when $CVb^2/CVa^2 > Mb/Ma$, both n and p can increase; when $CVb^2/CVa^2 = Mb/Ma$, only n can increase; when $CVb^2/CVa^2 < Mb/Ma$, neither n nor p can increase, implying an increase in q (although a pure increase in q occurs when $CVb^2/CVa^2 = 1$). In the case of LTD, in which a decrease in M is observed, this model represents complementary changes in the interpretation.

Solutions. Artificial CSF (ACSF) contained the following (in mM): 126 NaCl, 3 KCl, 25 $NaHCO_3$, 1 $NaHPO_4$, 2 $MgSO_4$, 2 $CaCl_2$, and 14 dextrose. The internal solution contained the following: 100 mM K-glutamate, 20 mM KCl, 10 mM K-HEPES, 4 mM Mg-ATP, 0.3 mM Na-GTP, 10 mM phosphocreatine, and 0.2% biocytin. The pH of the internal solution was adjusted to 7.35 with KOH, and the osmolarity was adjusted to 295 mOsm with sucrose. The drugs included 50 μM D-APV (Tocris Cookson) and 1 mM (*RS*)-($\pm$)-amino-4-carboxy-methyl-phenylacetic acid (MCPG) (Tocris Bioscience).

Results

Paired recording electrophysiology was used to analyze the development and plasticity of monosynaptic excitatory connections between pyramidal neurons in L4 of rat V1 (Maffei et al., 2004, 2006; Maffei and Turrigiano, 2008b). The basic properties of excitatory synapses were compared from P16 to P28, a developmental window straddling the transition from the precritical period to the peak of the critical period for visual cortical plasticity (Fagiolini et al., 1994; Feller and Scanziani, 2005). A total of 1585 monosynaptic pairs were tested, 260 of which were connected and 245 of which met the requirements for stable recordings: membrane potential of -60 mV or lower, series resistance no higher than 20 MΩ, and input resistance higher than 50 MΩ. Data were included in the analysis if these parameters did not change >10% during the course of the recording. Morphology and location of the recorded neurons was verified with *post hoc* reconstructions (Fig. 1*A*). The connection probability was remarkably stable across the developmental period under investigation (Fig. 1*C*; P16, 15.9%; P21, 18.6%; P25, 16.2%; P28, 23.9%; Pearson's χ^2 for contingency, $p = 0.27$). However, significant changes in baseline synaptic properties could be identified. As reported previously (Maffei and Turrigiano, 2008a), the amplitude of EPSP increased significantly from P16 to P21 (Fig. 1*B*,*C*; P16, 0.6 ± 0.05 mV, $n = 23$; P21, 0.9 ± 0.1 mV, $n = 32$; one-way ANOVA, $p < 0.01$; *post hoc t* test with Bonferroni's correction for multiple comparison, $p < 0.02$). After that, the average amplitude of synaptic responses remained stable up to P28 (Fig. 1*C*; P25, 1.1 ± 0.14 mV, $n = 18$; P28, 1.0 ± 0.22 mV, $n = 17$). There was also a significant decrease in the decay time constant of

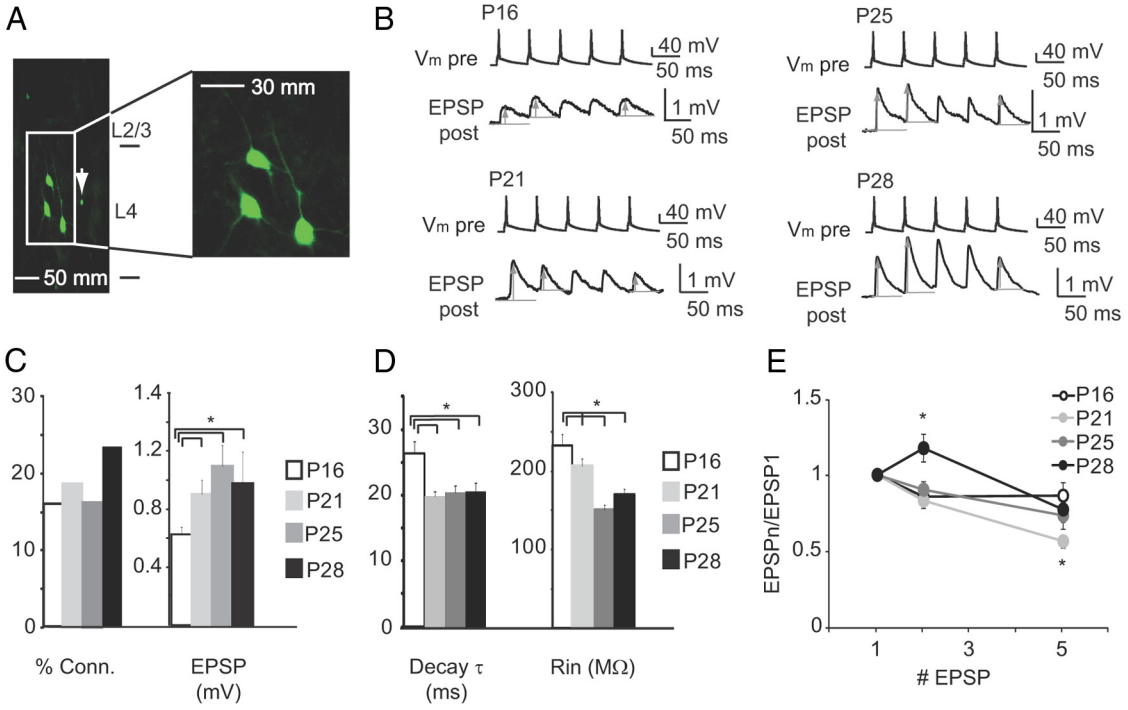

Figure 1. Maturation of recurrent excitatory synapses in L4. ***A***, Single-plane image of multiple patch-clamp recordings obtained from L4 of V1. Three of the four pyramidal neurons are visible in this single-plane image. The fourth neuron was on a different focal plane and can be visualized partially (see arrow). ***B***, Sample traces of monosynaptic connections recorded at different time points during the developmental window under study. Gray arrow, Peak of the EPSPs; gray lines, baseline for measurement of the amplitude of the first and subsequent EPSPs in the train. ***C***, Average data of connection probability (% Conn) and EPSP amplitude (EPSP) at P16 (white), P21 (light gray), P25 (dark gray), and P28 (black). ***D***, Average bar plot for EPSP decay time constants (Decay τ) and R_{in} at P16 (white), P21 (light gray), P25 (dark gray), and P28 (black). ***E***, Average short-term dynamics at P16 (white), P21 (light gray), P25 (dark gray), and P28 (black). Data are presented as ratio of the first EPSP in the train. In ***C–E***, data are presented as mean ± SE. Asterisks indicate significant differences.

monosynaptic EPSPs at the transition from P16 to P21, and after P21, the decay time constant remained stable (Fig. 1*D*; decay τ: P16, 26.4 ± 1.8 ms; P21, 19.8 ± 0.8 ms; P25, 20.4 ± 1.1 ms; P28, 20.6 ± 1.2 ms; one-way ANOVA P16–P28, $p < 10^{-4}$; one-way ANOVA P21–P28, $p = 0.8$). All of these changes were accompanied by a significant reduction in resting inputs resistance in the transition from P16–P21 to P25–P28 (Fig. 1*D*; R_{in}: P16, 232.9 ± 14.7 MΩ; P21, 206.8 ± 8.9 MΩ; P25, 150.9 ± 5.7 MΩ; P28, 170.3 ± 7.2 MΩ; one-way ANOVA, $p < 10^{-6}$; *post hoc t* test with Bonferroni's correction for multiple comparison, $p < 10^{-6}$).

Short-term dynamics of synaptic responses were also subject to developmental regulation. As shown in Figure 1*E*, the paired-pulse ratio (PPR) increased significantly at P28 (P16, 0.85 ± 0.05, $n = 23$; P21, 0.83 ± 0.05, $n = 32$; P25, 0.9 ± 0.06, $n = 18$; P28, 1.17 ± 0.09, $n = 17$; one-way ANOVA, $p < 10^{-3}$; *post hoc t* test with Bonferroni's correction for multiple comparison, $p < 0.01$). In addition, although monosynaptic excitatory connections were characterized by short-term depression in response to train of five presynaptic action potentials delivered at 20 Hz throughout the developmental window under analysis, the steady-state depression was more marked at P21 (Fig. 1*E*; EPSP5/EPSP1: P16, 0.86 ± 0.09; P21, 0.56 ± 0.04; P25, 0.73 ± 0.09; P28, 0.77 ± 0.08; one-way ANOVA, $p < 0.01$; *post hoc t* test with Bonferroni's correction for multiple comparison, $p < 0.01$). The developmental changes reported here are indicative of a set of maturation steps that involve both the presynaptic and the postsynaptic components of the synapse. Although significant changes in EPSP amplitude and EPSP decay time constant are specific to the precritical period, changes in EPSP short-term dynamics and resting input resistance (R_{in}) unfold at the transition into the critical period.

Mechanisms for spike-timing-dependent plasticity during the precritical period

Data from the rat barrel cortex indicate that the strength of L4 monosynaptic excitatory connections can be reduced by correlated presynaptic and postsynaptic firing in L4 of 2- to 3-week-old animals (Egger et al., 1999). We tested the possibility that spike-timing-dependent plasticity with properties similar to that of the barrel cortex might be induced in L4 of V1 during the same developmental time window. To do that, quadruple simultaneous patch-clamp whole-cell recordings were obtained from visually identified pyramidal neurons in L4 to isolate monosynaptic recurrent connections. A 10 min baseline was acquired by delivering trains of five action potentials at 20 Hz (repeated at 0.05 Hz) to measure the strength and dynamics of these connections. After that, bursts of 10 action potentials at 20 Hz were elicited in the presynaptic and postsynaptic pyramidal neuron using one of three delay time windows: −10, 0, and +10 ms, intervals that successfully changed the amplitude of EPSPs in the barrel cortex (Egger et al., 1999; Fig. 2*A*). During induction, the interburst interval was reduced from 20 to 10 s and the pairing of presynaptic and postsynaptic activity was repeated 20 times. As for the barrel cortex, in the developmental window from P16 to P21, all the tested pre-postsynaptic spiking delays resulted in a significant reduction of EPSP amplitude for every pair tested (Fig. 2*B*,*C*; $\Delta t = +10$ ms, −29.0 ± 9.9%, $n = 13$; $p < 0.01$; $\Delta t = 0$ ms, −32.9 ± 13.9%, $n = 5$; $p < 0.01$; $\Delta t = -10$ ms, −21.2 ± 7.6%, $n = 9$; $p < 0.01$; one-way ANOVA, $p = 0.5$). Spike-timing LTD reduced EPSP amplitude similarly at P16 and P21, indicating that this form of plasticity is reliably induced throughout the precritical period (Fig. 2*D*; P16, −38.0 ± 8.7%, $n = 8$; P21, −27.1 ± 5.9%, $n = 19$; $p = 0.5$). The magnitude of the depression did not

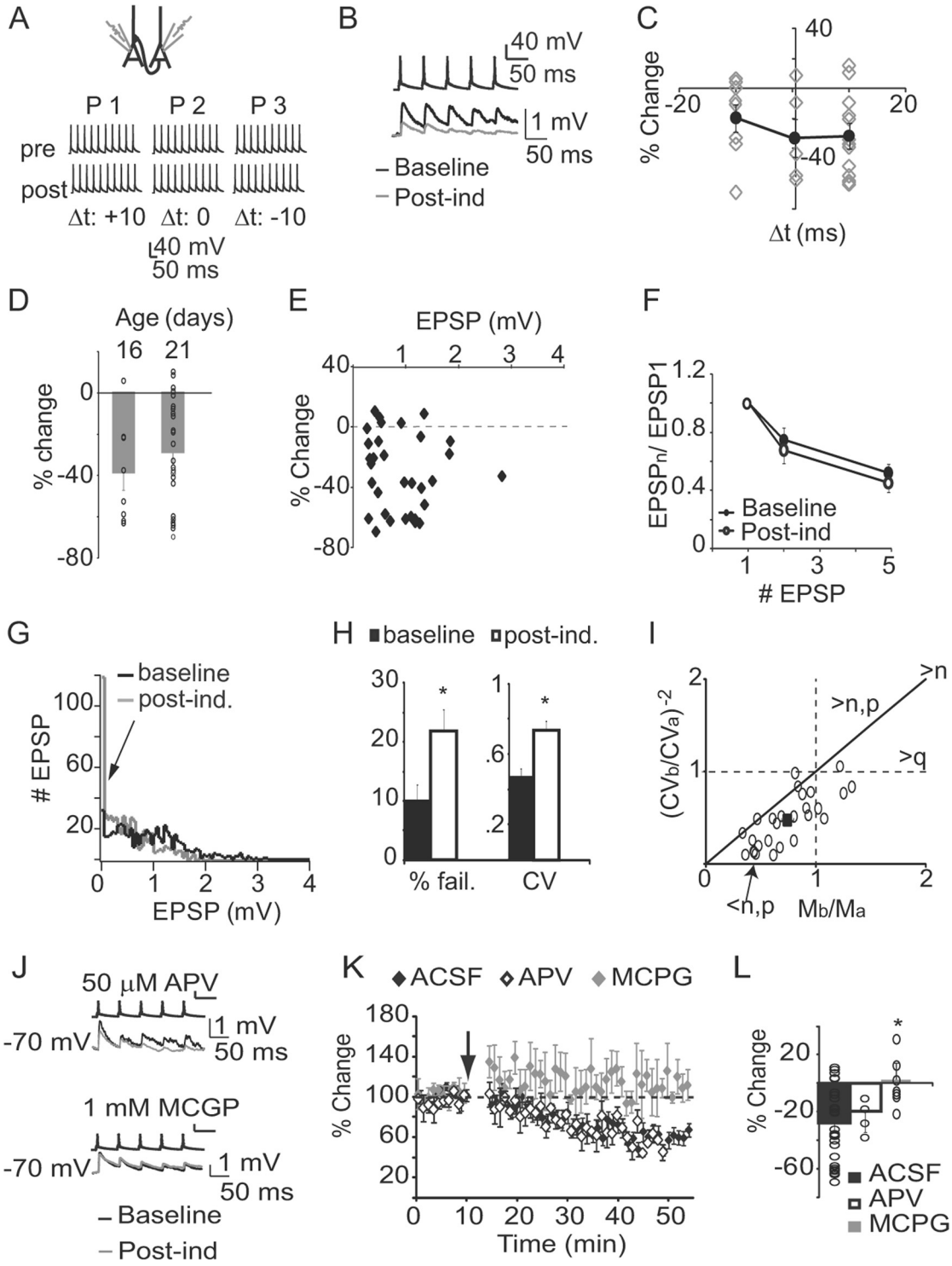

Figure 2. Spike-timing LTD in the precritical period. ***A***, Top, Experimental configuration. Bottom, Pairing paradigms for induction of plasticity. ***B***, Example traces showing significant decrease in EPSP amplitude after pairing (black, baseline; gray, after induction). ***C***, Magnitude of spike-timing LTD obtained with each pairing. Black circles, Average depression; gray diamonds, percentage depression for each pair recorded. The three different pairings were applied to different monosynaptic connections. ***D***, Average spike-timing LTD at P16 and P21. Data were obtained pooling the percentage changes obtained from all pairings at each age. Black circles, Percentage change for each pair at P16 and P21. ***E***, Magnitude of spike-timing LTD versus initial EPSP amplitude. ***F***, Average plot of short-term dynamics of EPSP amplitude (black, baseline; white, 40–50 min after induction). Inset, Average R_{in} at baseline (black) and after induction (white). ***G***, Distribution of EPSP amplitudes during baseline (black) and after induction (gray). Arrow indicates peak of subthreshold events. Bin size, 0.05 mV; detection threshold for EPSP, 0.15 mV. ***H***, Bar plot of average rates of failures (% fail) and *CV* before (black) and after (gray) induction. ***I***, Topographic representation of quantal analysis of EPSP amplitudes. Open circles, Data from each recorded pair; black square, average across all pairs. *CVa*, Baseline *CV*; *CVb*, post-induction *CV*; *Ma*, mean EPSP amplitude during baseline; *Mb*, mean EPSP amplitude after induction; *n*, number of release sites; *p*, release probability; *q*, quantal size; solid line, unity line. ***J***, Sample traces of the effect of APV (top) and MCPG (bottom) on the induction of spike-timing LTD (black, baseline; gray, 40–50 min after induction). Calibration for presynaptic spiking: 40 mV, 50 ms. ***K***, Time course of spike-timing LTD in ACSF (black), APV (white/black border), and MCPG (gray). Arrow, Time of induction. Data were averaged over 1 min and presented as percentage of control (100% = baseline). ***L***, Average percentage change in EPSP amplitude after induction in ACSF (black), APV (white/black border), and MCPG (gray). Black circles, Percentage change for each pair recorded in each condition. Data are presented as mean ± SE. Asterisks indicate significant differences.

correlate with the initial amplitude of the EPSP (Fig. 2*E*; $R^2 = 0.02$, $p = 0.4$) and was not accompanied by changes in PPR, short-term plasticity, and R_{in} (Fig. 2*F*; PPR baseline, 0.74 ± 0.08; PPR after induction, 0.68 ± 0.09; $p = 0.2$; EPSP5/EPSP1 baseline, 0.59 ± 0.05; EPSP5/EPSP1 after induction, 0.5 ± 0.04, $p = 0.2$; R_{in} baseline, 201.6 ± 25.2 MΩ; R_{in} after induction, 203.9 ± 25.4 MΩ; $p = 0.7$). To further address the site of expression of spike-timing LTD, failure rates and *CV* were quantified before and after induction (Fig. 2*G*,*H*). There was a shift to the left of the distributions of EPSP amplitudes after induction with a significant increase in peak of subthreshold events (Fig. 2*G*). Analysis of the rate of failures indicates that they increased significantly after induction (Fig. 2*H*; percentage failure: baseline, 10.3 ± 2.4%; after induction, 21.9 ± 3.7%; paired *t* test, $p < 10^{-3}$). In addition, the *CV* of EPSP amplitude was increased after induction (Fig. 2*H*; *CV*: baseline, 0.47 ± 0.04; after induction, 0.74 ± 0.05; paired *t* test, $p < 10^{-6}$). These data indicate that spike-timing LTD is likely expressed presynaptically. This hypothesis was further tested using quantal analysis with the methods described by Sola et al. (2004) to ask whether the decrease in EPSP amplitude induced by the spike-timing paradigm was attributable to a decrease in probability of release (p), quantal size (q), or number of release sites (n) (Sola et al., 2004). As shown in Figure 2*I*, the distribution of data fell in the quadrant indicating a decrease in n or p. Together with the reduction in failure rates, these data are consistent with a presynaptic site of expression for spike-timing LTD. Additional expression mechanisms cannot be excluded by our analysis. Particularly the lack of changes in PPR and the results of the quantal analysis suggest that, besides reduced release probability, silencing of functional synaptic sites may be involved.

This form of spike-timing LTD was not blocked by bath application of the NMDAR antagonist APV (50 μM; Fig. 2*J–L*; APV, −24.8 ± 6.3%, $n = 4$). In addition, application of APV did not change the amplitude of baseline EPSPs, indicating that these receptors do not contribute significantly to the recurrent monosynaptic response recorded at −70 mV at this time in development (ACSF, 0.9 ± 0.1 mV, $n = 32$; APV, 1.2 ± 0.3 mV; unpaired *t* test, $p = 0.22$). Although spike-timing LTD appears to be independent of NMDAR activation, perfusion of the mGluR blocker MCGP (1 mM) prevented its induction (Fig. 2*J–L*; MCPG, 6 ± 12.4%, $n = 7$; paired *t* test, $p = 0.51$). The PPR and steady-state ratio before and after induction in the presence of MCPG were also unchanged (MCPG, PPR baseline, 0.74 ± 0.12; PPR after induction, 0.69 ± 0.1; $n = 7$; paired *t* test, $p = 0.69$; MCPG, EPSP5/EPSP1 baseline, 0.56 ± 0.08; EPSP5/EPSP1 after induction, 0.48 ± 0.05; paired *t* test, $p = 0.38$). These data indicate that spike-timing-dependent plasticity is reliably induced in L4 of V1 during the precritical period. Similar to previous findings in the barrel cortex, spike-timing LTD in L4 requires the activation of mGluRs and is expressed presynaptically.

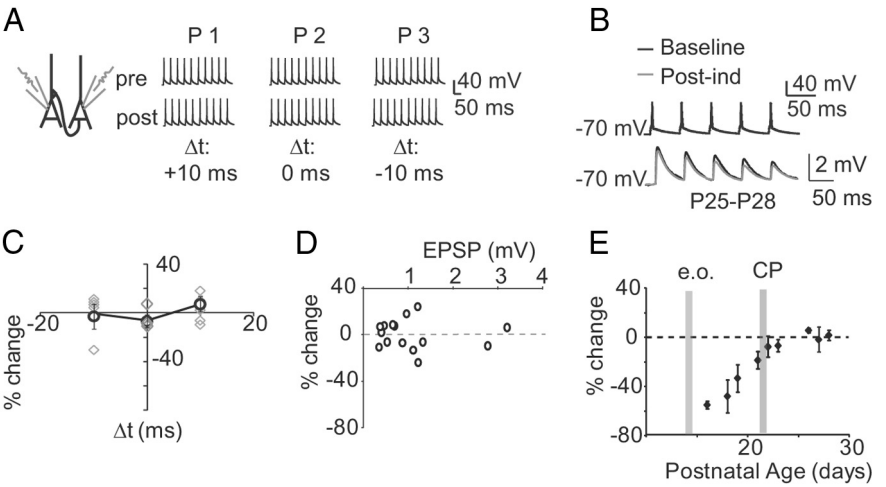

Figure 3. Spike-timing LTD induction fails after the opening of the critical period. ***A***, Left, Experimental configuration. Right, Pairing paradigms used for induction. ***B***, Sample traces of EPSP recorded at P25–P28. Baseline, Black; after induction, gray. ***C***, Magnitude of changes in EPSP amplitude in response to each pairing. White circles, Average percentage change for each pairing; gray diamonds, percentage change for each connection. The three pairings were applied to different connections. ***D***, Distribution of the percentage change for each pair plotted against the initial EPSP showing lack of correlation. ***E***, Average percentage change induced by presynaptic and postsynaptic correlated firing for all of the ages tested during the developmental window under analysis. The gray bars indicate important developmental milestones: e.o., eye opening; CP, opening of the critical period. Data are presented as mean ± SE.

Spike-timing-dependent plasticity is lost in the critical period

Because timing between inputs is an important factor in visual cortical development (Castelo-Branco et al., 1998; Weliky, 2000), one would expect that spike-timing LTD might be induced reliably in L4 also later in development. To test this possibility, spike-timing LTD was induced at monosynaptic connections between L4 pyramidal neurons in acute slices from P25–P28 rats. As shown in Figure 3, spike-timing-dependent pairing of presynaptic and postsynaptic activity failed to change the amplitude of monosynaptic EPSPs at any timing interval tested (Fig. 3*B*,*C*; $\Delta t = -10$ ms, 7.2 ± 6.3%, $n = 6$; $\Delta t = 0$, −3.8 ± 4.4%, $n = 3$; $\Delta t = -10$ ms, −2.9 ± 9.5, $n = 5$; one-way ANOVA, $p = 0.6$). The initial amplitude of the EPSP did not correlate with the induction of plasticity (Fig. 3*D*; $R^2 = 0.01$, $p = 0.7$). There was no significant change in PPR, short-term plasticity and R_{in} during the recordings (PPR baseline, 1.0 ± 0.06; PPR after induction, 0.9 ± 0.15; $p = 0.2$; EPSP5/EPSP1 baseline, 0.7 ± 0.05; EPSP5/EPSP1 after induction, 0.68 ± 0.04; paired *t* test, $p = 0.23$; R_{in} baseline, 160.7 ± 9.7 MΩ; R_{in} after induction, 177.1 ± 14.3 MΩ; $p = 0.3$). Figure 3*E* summarizes the magnitude of spike-timing LTD changes from P16 to P28. These results indicate that spike-timing LTD in L4 of V1 is limited to the developmental window preceding the critical period for visual cortical plasticity. Thus, spike-timing-dependent plasticity at L4 recurrent synapses may be important for the early stages of circuit refinement, but it is unlikely critical for the processes taking place after P21.

Multiple mechanisms for plasticity at L4 recurrent excitatory synapses

Is spike-timing-dependent plasticity during the precritical period the only mechanism for plasticity at recurrent excitatory synapses in L4? And is L4 excitatory plasticity lost by the end of the third postnatal week? We tested the possibility that L4 excitatory neurons may have a second set of mechanisms for plasticity that may allow them to be plastic later in development. To do that, a plasticity induction paradigm was designed to mimic presynaptic spiking on the upstate of a slow wave, a pattern of activity similar

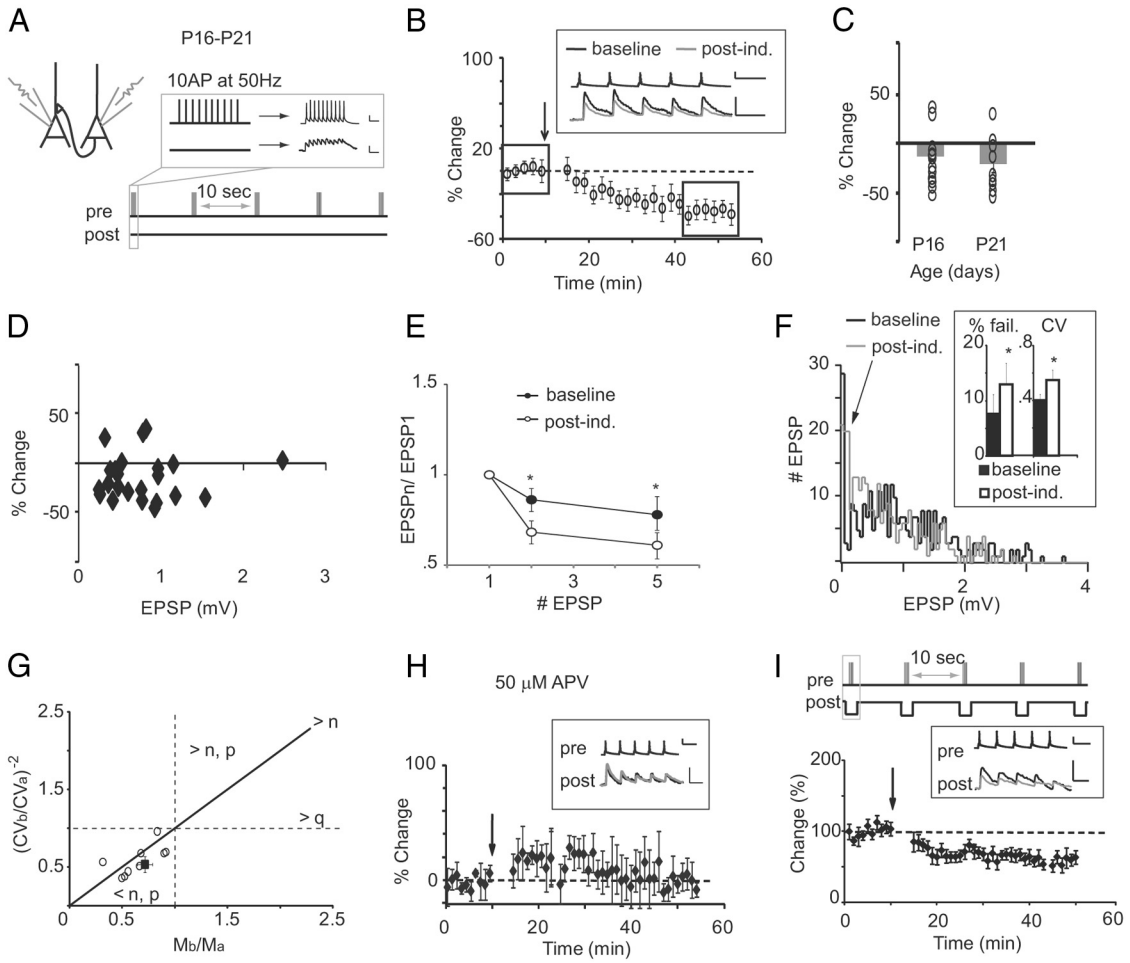

Figure 4. Slow-wave LTD during the precritical period. ***A***, Top left, Recording configuration. Bottom, Induction paradigm. Inset, Enlargement of the diagram indicating presynaptic burst (left) and sample trace of presynaptic and postsynaptic membrane potential during the burst (right). ***B***, Time course of EPSP amplitude. Arrow, Time of induction. Each point is the average change of EPSP amplitude over 2 min of recordings (100% = baseline). The squares represent the time points used for quantifying the magnitude of slow-wave LTD. The inset shows a sample recording. Black, Baseline; gray, after induction. Calibration: presynaptic neuron, 40 mV, 50 ms; postsynaptic neuron, 1 mV, 50 ms. ***C***, Average change in EPSP amplitude. Black circles, Percentage change in EPSP amplitude for each recorded pair. ***D***, Plot of percentage changes in EPSP amplitude relative to the initial amplitude of EPSPs recorded for each monosynaptic connection. ***E***, Ratio of EPSP2/EPSP1 and EPSP5/EPSP1 at baseline (black) and after induction (white). ***F***, Distribution of EPSP amplitudes before (black) and after (gray) induction of slow-wave LTD. Arrow, Subthreshold events; bin size, 0.05 mV; threshold for EPSP detection, 0.15 mV. Inset, Bar plot of failure rates (% fail.) and *CV* in baseline (black) and after induction (white/black border). ***G***, Topographic representation of quantal analysis. *CVa*, Baseline *CV*; *CVb*, after induction *CV*; *Ma*, average baseline EPSP; *Mb*, average post-induction EPSP. Note that the data point falls in the area of decreased *n* or *p* ($<n, p$). ***H***, Time course of slow-wave LTD in the presence of 50 μM APV. The arrow indicates the time of induction. Inset, Left, Sample traces before (black) and after (gray) induction. Calibration: top, 40 mV, 50 ms; bottom, 1 mV, 50 ms. ***I***, Top, Diagram of induction paradigm. Note that the postsynaptic neuron is hyperpolarized coincident with the presynaptic bursts. Bottom, Time course of slow-wave LTD induced with the paradigm above. Inset, Sample traces of presynaptic (top) and postsynaptic (bottom) recordings. Baseline, Black; after induction, gray. Calibration in inset: presynaptic neuron, 40 mV, 50 ms; postsynaptic neuron, 1 mV, 50 ms. Data are presented as mean and SE; asterisks indicate significant differences. AP, Action potential.

to that observed in developing visual cortical neurons (Rochefort et al., 2009). The induction paradigm consisted of 20 brief bursts of 10 action potentials at 50 Hz separated by a 10 s interval (0.1 Hz; see Materials and Methods and Fig. 4*A*). To mimic sparseness, the postsynaptic neuron was sitting at −70 mV in current clamp, and its membrane potential was free to depolarize in synch with presynaptic bursts (Fig. 4*A*, inset). Paired recordings were obtained from visually identified pyramidal neurons in L4 of V1. Once a monosynaptic connection was detected, a 10 min baseline was recorded by eliciting five action potentials at 20 Hz in the presynaptic neuron and recording EPSPs from the postsynaptic neuron in current clamp (at 0.05 Hz; small direct currents were injected at the beginning of the recording to adjust the membrane potential to −70 mV for uniform comparisons of changes in EPSP amplitude after induction of plasticity; see Materials and Methods). After baseline acquisition, the induction paradigm was applied. The induction lasted a total of 3 min 25 s. In the developmental window from P16 to P21, this pattern of activity induced LTD (slow-wave LTD; Fig. 4*B*,*C*; $-25.27 \pm 6.31\%$; $n = 22$; paired t test, $p < 10^{-3}$). The magnitude of the depression was not correlated with the initial amplitude of monosynaptic EPSPs (Fig. 4*D*; LTD vs baseline EPSP, $R^2 = 0.05$, $p = 0.8$). After induction of slow-wave LTD, there was a significant decrease in PPR and an increase in short-term depression, as indicated by the significant decrease in steady-state ratio (Fig. 4*E*,*F*; PPR: baseline, 0.84 ± 0.04; after induction, 0.7 ± 0.05; $n = 22$; paired t test, $p < 0.001$; EPSP5/EPSP1: baseline, 0.6 ± 0.04; after induction, 0.4 ± 0.03; $n = 22$; paired t test, $p < 10^{-5}$). No changes in R_{in} were observed (Fig. 4*F*; R_{in} baseline, 250.8 ± 17.3 MΩ; R_{in} after induction, 256.1 ± 16.7 MΩ; $n = 22$, $p = 0.5$).

A decrease in PPR after slow-wave LTD was attributable to a significantly larger depression of the second EPSP in the train (average reduction of EPSP1, $24.9 \pm 9.1\%$; average reduction of EPSP2, $38.2 \pm 8.1\%$; paired t test, $p < 0.01$). These data indicate

that each subsequent presynaptic action potential in a train of stimuli elicits an increasingly stronger depression of subsequent EPSPs. This effect suggests that the depression of EPSP amplitude observed after slow-wave LTD induction may depend on reduced release probability but may also involve other presynaptic changes, such as depletion of synaptic resources or refractoriness of the release machinery, resulting in reduced neurotransmitter release. To verify this hypothesis, we analyzed the distribution of EPSP amplitudes before and after induction and quantified a number of parameters that are reliably used to investigate the site of expression of long-term synaptic plasticity. There was a shift to the left of the entire distribution of EPSP amplitudes after induction, with an apparent increase of the number of subthreshold events suggesting a possible increase in the rate of failures (Fig. 4*F*, arrow). To confirm this, we quantified the failure rates and *CV* of monosynaptic EPSPs before and after induction of slow-wave LTD (Fig. 4*F*, inset). There was a significant increase in failure rates and *CV* after slow-wave LTD induction (Fig. 4*F*, inset; percentage failures: baseline, 8 ± 3%; after induction, 13 ± 4; paired *t* test, $p < 0.05$; *CV*: baseline, 0.4 ± 0.04; after induction, 0.6 ± 0.07; paired *t* test, $p < 0.003$). To further test the potential mechanisms of expression of slow-wave LTD, we performed quantal analysis (Sola et al., 2004). Figure 4*G* shows that slow-wave LTD depends on a significant decrease in *n*, *p*, or both, indicating that changes in presynaptic release, attributable to either reduced release probability or reduced number of release sites, are involved in the expression of slow-wave LTD. These data support the interpretation that slow-wave LTD is expressed presynaptically, similarly to spike-timing LTD. A feature that is specific to slow-wave LTD, however, is that depression is more pronounced in subsequent EPSPs in a train of stimuli, causing a reduction in PPR. Thus, although both forms of plasticity have a presynaptic site of expression, the specific mechanisms involved in regulating synaptic release after induction of these two forms of LTD might differ significantly.

We investigated the mechanisms required for the induction of plasticity after slow-wave presynaptic bursting to ask whether they share similarities with those involved in spike-timing LTD. Bath application of the NMDAR blocker APV (50 μM) did not change the baseline amplitude of monosynaptic EPSPs but impaired slow-wave LTD (Fig. 4*H*; EPSP baseline, 0.76 ± 0.11 mV, $n = 22$; baseline APV, 0.72 ± 0.15 mV, $n = 8$; paired *t* test, $p = 0.9$; average LTD APV, −8.6 ± 11.9%, $n = 8$; unpaired *t* test, $p = 0.8$). NMDAR blockade not only prevented the depression of EPSP amplitude but impaired the decrease in PPR and short-term plasticity that are associated with slow-wave LTD (Fig. 4*H*, inset; PPR: APV baseline, 0.76 ± 0.09; APV after induction, 0.7 ± 0.06; $n = 8$; paired *t* test, $p = 0.4$; EPSP5/EPSP1: APV baseline, 0.5 ± 0.07; APV after induction, 0.45 ± 0.06; $n = 8$; paired *t* test, $p = 0.36$).

Previous data indicate that, in visual cortex, LTD may depend on the activation of NMDARs located presynaptically (Sjöström et al., 2003). To investigate whether presynaptic NMDARs are involved in slow-wave LTD, we paired the slow-wave induction paradigm with hyperpolarization of postsynaptic membrane potential to −90 mV (300 ms; see diagram in Fig. 4*I*). Such hyperpolarization would prevent the release of the magnesium block, thus precluding the activation of postsynaptic NMDARs during presynaptic bursting. Slow-wave LTD was still reliably induced, supporting the interpretation that this form of plasticity depends on the activation of NMDARs located on the presynaptic neuron (Fig. 4*I*; percentage change, −31.6 ± 5.6%; $n = 12$; $p < 0.01$). This paradigm of LTD induction produced also the decrease in PPR and steady-state ratio that are typical of slow-wave LTD, confirming that the same form of LTD was induced even when the postsynaptic neuron was hyperpolarized (PPR: baseline, 0.76 ± 0.07; after induction, 0.6 ± 0.04; $p = 0.01$; EPSP5/EPSP1: baseline, 0.45 ± 0.04; after induction, 0.34 ± 0.04; $p = 0.005$). Together, these data indicate that, during the precritical period, different patterns of presynaptic and postsynaptic activity (spike-timing and slow-wave presynaptic bursting) can engage different mechanisms in the induction and expression of LTD at L4 recurrent excitatory synapses.

A switch in sign of plasticity correlates with the critical period for visual cortical plasticity

Slow-wave presynaptic bursting had a dramatically different effect at L4 recurrent synapses during the critical period. In the developmental time window from P25 to P28, the slow-wave bursting paradigm described above induced a significant potentiation of recurrent EPSP amplitude (slow-wave LTP: +44.17 ± 16.35%, $n = 20$, $p = 0.014$; Fig. 5*B*,*C*). The magnitude and success rate of potentiation were independent of baseline EPSP amplitude (Fig. 5*D*; LTP vs baseline EPSP, $R^2 = 0.15$, $p = 0.7$). After potentiation, there was a significant decrease in PPR and an increase in short-term depression in response to trains of presynaptic spikes at 20 Hz (Fig. 5*E*; PPR: baseline, 1.09 ± 0.08; after induction, 0.94 ± 0.05; $n = 20$; paired *t* test, $p < 10^{-4}$; EPSP5/EPSP1: baseline, 0.75 ± 0.06; after induction, 0.5 ± 0.04, $n = 22$; paired *t* test, $p < 10^{-6}$). No change was observed in R_{in} after induction of slow-wave LTP (baseline, 157.1 ± 7.8 MΩ; after induction, 166.0 ± 7.3 MΩ; paired *t* test, $p = 0.41$). A decrease in PPR is consistent with the possibility that slow-wave LTP was expressed presynaptically. The involvement of potential presynaptic changes was further indicated by a shift to the right of the entire distribution of EPSP amplitudes and by a reduction of the number of events below threshold (Fig. 5*F*; threshold, 0.15 mV). To confirm the presynaptic site of expression of slow-wave LTP, we quantified potential changes in failure rates and *CV* after induction. As shown in the inset in Figure 5*F*, there was a significant decrease in failure rates and *CV* (failure rate: baseline, 6 ± 2%; after induction, 2 ± 1%; paired *t* test, $p < 0.05$; *CV*: baseline, 0.6 ± 0.04; after induction, 0.4 ± 0.03; paired *t* test, $p < 0.03$). The indication that presynaptic changes may be involved in the expression of slow-wave LTP was further confirmed by quantal analysis. Figure 5*G* shows the results of quantal analysis indicating that there was a significant increase in presynaptic release after induction that was attributable to either increased probability of release or increase in the number of release sites.

The mechanisms for slow-wave LTP were tested to assess whether they shared similarities with those involved in the slow-wave LTD observed in the precritical period. Bath application of APV decreased the baseline EPSP amplitude, indicating that at this time in development NMDARs account for a significantly larger portion of the EPSP, even at the membrane potential of −70 mV used for these experiments (baseline EPSP, 1.01 ± 0.17 mV, $n = 21$; APV EPSP, 0.6 ± 0.09 mV, $n = 6$; unpaired *t* test, $p < 0.03$). This effect is specific to the P25–P28 time window because we did not observe any effect of APV on baseline amplitude in younger animals. The effect of APV on EPSP amplitude was not associated with changes in PPR and short-term depression (baseline PPR, 1.07 ± 0.09; APV PPR, 0.95 ± 0.08; unpaired *t* test, $p = 0.5$; baseline EPSP5/EPSP1, 0.75 ± 0.06; APV EPSP5/EPSP1, 0.73 ± 0.07; unpaired *t* test, $p = 0.6$). NMDAR blockade impaired the induction and expression of slow-wave LTP, pre-

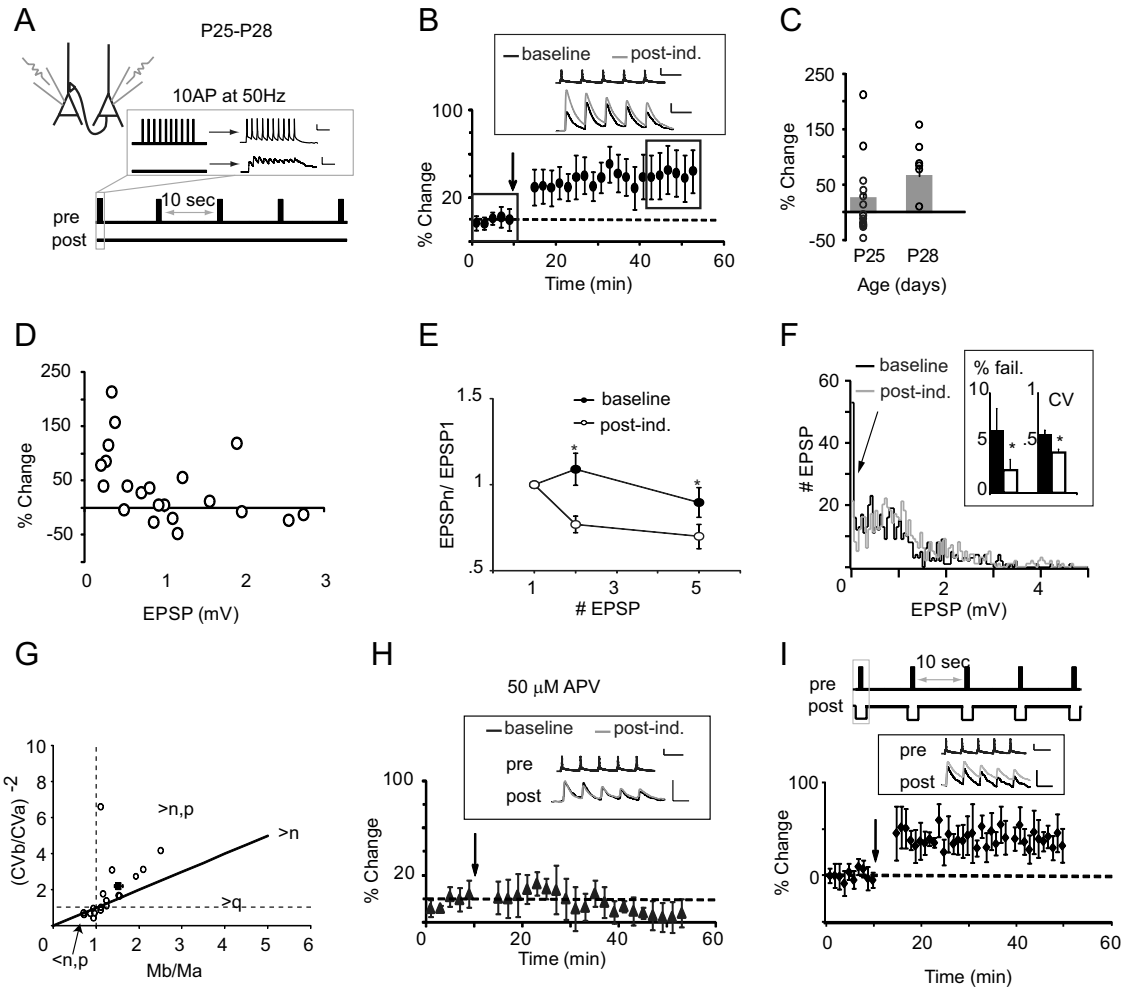

Figure 5. Switch in sign of plasticity in the critical period. ***A***, Top, Recording configuration. Bottom, Induction paradigm. Inset, Left, Enlargement of the portion of the diagram indicated by the gray rectangle; right, sample trace of presynaptic and postsynaptic activity during an induction burst. Calibration: presynaptic neuron, 20 mV, 50 ms; postsynaptic neuron, 0.5 mV, 50 ms. ***B***, Time course of slow-wave LTP at P25–P28. Arrow, Time of induction; squares, time points at which data were compared. Each data point is averaged over 2 min of recordings. The inset shows sample traces averaged during baseline (black) and 40–50 min after induction (gray). Calibration in the inset: presynaptic neuron, 40 mV, 50 ms; postsynaptic neuron, 1 mV, 50 ms. ***C***, Bar plot of average percentage changes in EPSP amplitude after induction of plasticity at P25 and P28. The circles indicate percentage change in EPSP amplitude of each pair. ***D***, Plot of percentage changes in EPSP amplitude versus the initial EPSP amplitude for each pair. ***E***, Short-term dynamics of EPSP amplitude during baseline (black circles) and after LTP induction (open circles). ***F***, Distribution of EPSP amplitudes before (black) and after (gray) induction of slow-wave LTP. Arrow, Subthreshold events; bin size, 0.05 mV; detection threshold for EPSP, 0.15 mV. Inset, Average failure rate (% fail) and *CV* before (black) and after (white) induction. ***G***, Topographic representation of quantal analysis. Open circles, Data from each recorded pair; black square, average value. The black line represents the unity line. ***H***, Time course of slow-wave LTP induced in the presence of 50 μ_M APV. Inset, Sample traces of monosynaptic EPSP recorded before (black) and after (gray) induction. Calibration: top, 40 mV, 50 ms; bottom, 1 mV, 50 ms. ***I***, Top, Diagram of induction paradigm. Note that the postsynaptic neuron is hyperpolarized coincident with the presynaptic bursts. Bottom, Time course of slow wave LTP induced with the paradigm above. Arrow indicates the time of induction. Inset, Sample traces of presynaptic and postsynaptic activity before (black) and after (gray) induction. Calibration: presynaptic neuron, 40 mV, 50 ms; postsynaptic neuron, 1 mV, 50 ms. Data are presented as mean ± SE. Asterisks indicate significant differences. AP, Action potential.

vented the reduction in PPR, and impaired changes in short-term plasticity (Fig. 5*H*; LTP APV, 5.4 ± 7.7%, $n = 6$, $p = 0.5$; PPR APV: baseline, 0.95 ± 0.08; after induction, 0.8 ± 0.06; paired *t* test, $p = 0.21$; EPSP5/EPSP1 APV: baseline, 0.73 ± 0.07; after induction, 0.53 ± 0.05; paired *t* test, $p = 0.11$). These data indicate that slow-wave LTP depends on the activation of NMDARs. The location of NMDARs involved in slow-wave LTP is unknown. We tested the possibility that slow-wave LTP may depend on the activation of presynaptic NMDARs by pairing each presynaptic burst in the induction paradigm with hyperpolarizing steps to −90 mV (see diagram in Fig. 5*I*) injected in the postsynaptic neuron. In these experimental conditions, slow-wave LTP was still successfully induced, suggesting that the NMDARs involved in the induction of this form of plasticity are likely located presynaptically (Fig. 5*I*; percentage change: EPSP, 29.5 ± 8.2%, $n = 10$; $p < 0.008$). The changes in PPR and steady-state ratio associated with slow-wave LTP were also maintained (PPR: baseline, 1.06 ± 0.1; after induction, 0.8 ± 0.06; $p = 0.018$; steady-state ratio: baseline, 0.74 ± 0.1; after induction, 0.56 ± 0.07; $p = 0.028$).

Our findings demonstrate that the maturation of L4 recurrent excitatory synapses leads to a switch in sign of plasticity from LTD in the precritical period to LTP in the critical period. Both forms of plasticity depend on the activation of presynaptic NMDARs and show a presynaptic site of expression. The switch in sign of plasticity correlates with a developmentally regulated increase in the contribution of NMDARs to monosynaptic recurrent EPSPs. These data show for the first time that, in L4 of V1, synaptic plasticity can be induced beyond eye opening and that presynaptic NMDARs are crucial regulators of both LTP and LTD. In

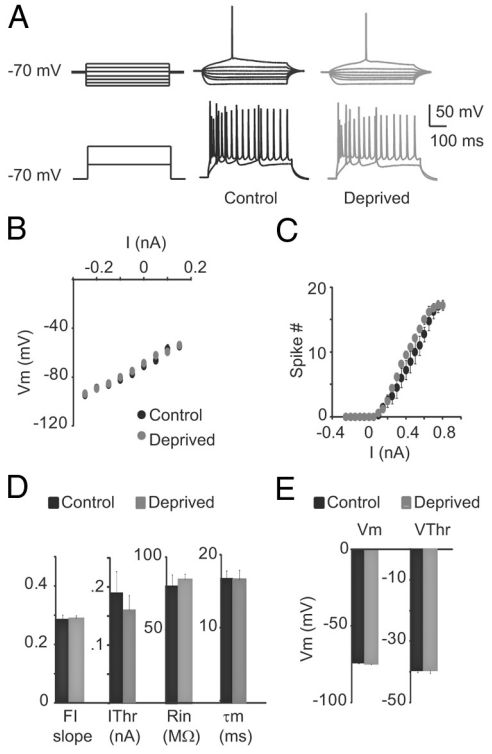

Figure 6. MD did not induce changes in intrinsic excitability in L4 pyramidal neurons. ***A***, Sample traces of membrane potential in response to current injections. Top, Left, Subthreshold current injections (current steps, 0.05 nA). Middle, Membrane potential in response to subthreshold current injections in control slices. Right, Membrane potential in response to subthreshold current injections in deprived slices. Bottom, Left, Suprathreshold current injections (selected current steps, 0.3 and 0.8 nA). Middle, Membrane potential in response to suprathreshold current injections in control slices. Right, Membrane potential in response to suprathreshold current injections in deprived slices. ***B***, Membrane voltage in response to subthreshold current injections in control (black) and deprived (gray) slices. ***C***, Plot of the number of action potentials versus current injections in control (black) and deprived (gray) slices. ***D***, Bar plot of average values for the slope of the frequency–current curve (FI slope), current to threshold (I_{thr}), R_{in}, and τ_m in control (black) and deprived (gray) slices. ***E***, Bar plot of average resting membrane potential (V_m) and action potential threshold (V_{thr}) in control (black) and deprived (gray) slices. Data are mean ± SE. Asterisks indicate significant differences.

addition, our findings highlight the importance of the process of maturation of cellular properties in the induction of different forms of plasticity in developing visual cortex.

Visual deprivation does not affect intrinsic excitability but impairs slow-wave LTP

The specificity of slow-wave LTP for the critical period, a window in development in which circuits are particularly sensitive to changes in sensory input, suggests that changes in visual drive may affect this form of plasticity. To test this possibility, we sutured one eye shut to P24 ± 1 d in rats and maintained the MD until P28 ± 1 d. Recordings were performed in the monocular region of the hemispheres contralateral (deprived) and ipsilateral (control) to the deprived eye. Four-day-eyelid closure did not affect the intrinsic properties of L4 pyramidal neurons. Figure 6 shows that there was no significant difference in the voltage versus current relationship in the subthreshold range (Fig. 6*B*). Neurons from control and deprived slices responded with a similar number of action potentials to suprathreshold current injections (Fig. 6*C*). The slope of the frequency versus current injection was also similar (Fig. 6*D*; frequency–current slope: control, 0.28 ± 0.02, $n = 5$; deprived, 0.29 ± 0.01, $n = 7$; unpaired t test, $p = 0.8$). The current to threshold was not significantly different in the two conditions (Fig. 6*D*; I_{thr}: control, 0.19.0 ± 3.7 nA; deprived, 16.0 ± 3.5; $p = 0.5$). The R_{in} and membrane time constant (τ_m) were unchanged (Fig. 6*D*; R_{in}: control, 80.1 ± 8.2 MΩ; deprived, 84.6 ± 3.9 MΩ; $p = 0.6$; τ_m: control, 17.1 ± 1.0 ms; deprived, 16.9 ± 1.2 ms; $p = 0.9$). There was no difference in resting membrane potential and in the spike threshold measured as the interpolated membrane potential at which dV/dt was 20 V/s (Fig. 6*E*; resting membrane potential, V_m: control, −73.0 ± 0.7 mV; deprived, −73.9 ± 0.5 mV; $p = 0.4$; spike threshold, V_{thr}: control, −39.3 ± 3.7 mV; deprived, −39.2 ± 1.0 mV; $p = 0.9$). Together, these data demonstrate that 4 d visual deprivation during the critical period does not affect the intrinsic properties of L4 pyramidal neurons.

We then analyzed the effect of MD on baseline synaptic properties. Four-day MD did not affect the probability of finding connected pairs in the P25–P28 time window (Fig. 7*B*; percentage connected: control, 11 of 42 tested, 26.2%; deprived, 32 of 114 tested, 28.1%; χ^2 for contingency, $p = 0.9$). Furthermore, the baseline EPSP amplitude, decay time constant, and short-term dynamics were unaltered (Fig. 7*A*,*B*; EPSP: control, 0.77 ± 0.19 mV, $n = 11$; deprived, 0.76 ± 0.13 mV, $n = 32$; unpaired t test, $p = 0.98$; decay τ: control, 19.6 ± 1.9 ms; deprived, 21.1 ± 1.1 ms; unpaired t test, $p = 0.47$; PPR: control, 1.06 ± 0.06; deprived, 0.96 ± 0.1; $p = 0.44$; EPSP5/EPSP1: control, 0.68 ± 0.12; deprived, 0.77 ± 0.09; unpaired t test, $p = 0.5$). These data demonstrate that MD does not directly affect the strength and intrinsic properties of recurrent monosynaptic connections between L4 pyramidal neurons.

In a subset of lid-sutured rats ($n = 5$ rats), we tested whether MD affected the induction of slow-wave LTP. Four-day MD impaired slow-wave LTP in slices from the hemisphere contralateral to the deprived eye. The same pattern of stimulation induced LTD instead (Fig. 7*C*,*D*; control, 41.25 ± 9.4% of baseline; $n = 9$ connected pairs; deprived, −11.6 ± 7.33% of baseline, $n = 10$ connected pairs; unpaired t test, $p < 10^{-3}$). After induction, the PPR remained unchanged, indicating that changes in paired-pulse depression are specific to slow- wave-LTP (PPR: deprived baseline, 0.96 ± 0.1, $n = 10$; deprived after induction, 0.85 ± 0.1; unpaired t test, $p = 0.28$). The changes in short-term plasticity that are observed after slow-wave LTP induction were also prevented by MD, as indicated by the lack of changes in steady-state ratio of EPSP amplitudes in response to a train of five action potentials at 20 Hz (EPSP5/EPSP1: control baseline, 0.78 ± 0.09; control after induction, 0.54 ± 0.14; $n = 9$; paired t test, $p < 10^{-4}$; deprived baseline, 0.68 ± 0.12; deprived after induction, 0.62 ± 0.18; paired t test, $p = 0.49$). Thus, visual experience is necessary for the engagement of mechanisms involved in the induction and expression of slow-wave LTP during the critical period.

Discussion

In this set of experiments, we investigated the plasticity associated with circuit maturation and refinement at L4 recurrent excitatory synapses. We have shown that: (1) recurrent excitatory synapses in L4 are endowed with multiple mechanisms for plasticity; (2) there is a sharp, developmentally regulated switch in sign and mechanisms for plasticity during postnatal development; and (3) visual experience is necessary for the switch in sign and mechanisms for excitatory synaptic plasticity.

The results presented here indicate that, although the connection probability remains stable throughout the time window under study, the process of maturation of recurrent excitatory

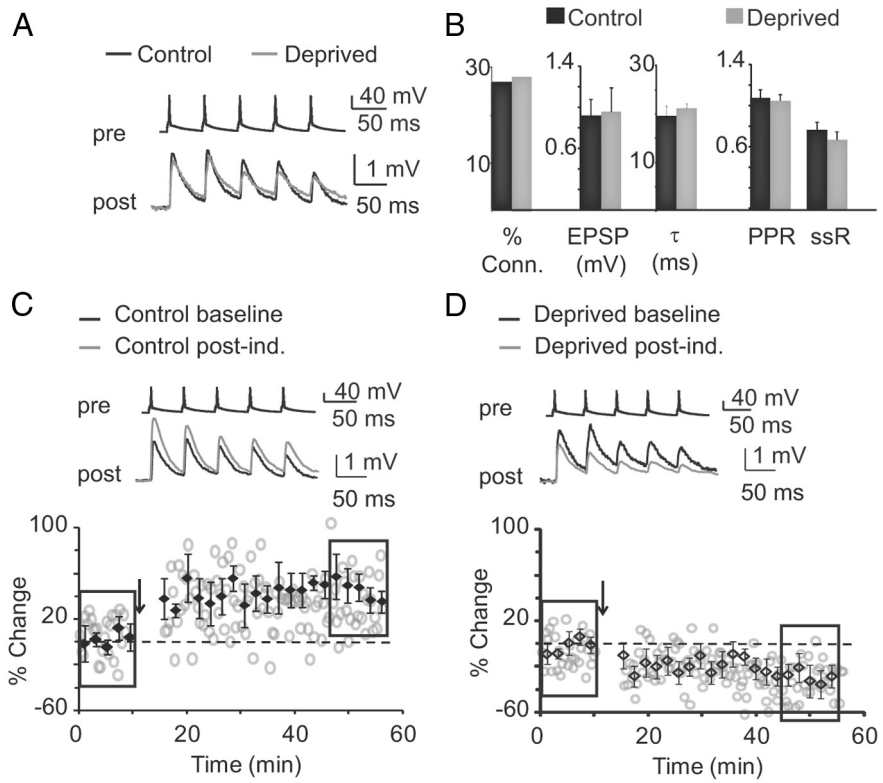

Figure 7. Visual experience is necessary for the induction of slow-wave LTP during the critical period. ***A***, Sample traces of monosynaptically connected pairs of neurons from the monocular region of the hemisphere ispilateral (control; black) and contralateral (deprived; gray) to the closed eye. ***B***, Baseline properties of monosynaptic connections in control (black) and deprived (gray) hemispheres (% Conn, connection probability; EPSP, EPSP amplitude; τ, decay time constant; ssR, steady-state ratio). ***C***, Top, Sample traces of monosynaptic connections from the control hemisphere. Black, Baseline; gray, after induction. Bottom, Time course of EPSP amplitude during the recordings. Rectangles indicate the time points used to quantify average baseline and magnitude of slow-wave LTP. The arrow indicates the time of induction. ***D***, Top, Sample traces of monosynaptic connections recorded in the deprived hemisphere. Black, Baseline; gray, after induction. Bottom, Time course of EPSP amplitude during the recordings. Rectangles indicate the time points used to quantify average baseline and magnitude of LTP. The arrow indicates the time of induction. Data are presented as mean ± SE. Asterisks indicate significant differences.

synapses in L4 occurs through a sequence of transitions that involve both presynaptic and postsynaptic components of the connection. The first steps in the process of maturation account for the acquisition of larger and faster decaying EPSPs, as well as increased short-term depression in the time window from P16 to P21. Increased amplitude and short-term depression suggest a developmental regulation of release probability. A decrease in EPSP decay time constant may be attributable to changes in NMDAR subunit composition, a process that precedes the opening of the critical period (Quinlan et al., 1999; Roberts and Ramoa, 1999; Chen et al., 2000; Erisir and Harris, 2003). Both these events occurred before P21, after that, EPSP amplitude and decay remained stable. Although we do not observe any additional decrease in EPSP decay time constant from P21 to P25, our recordings were performed at a holding potential of −70 mV. The possibility that an additional decrease in decay time constant may occur if recordings were performed at more depolarized membrane potentials—at which NMDAR contribution to the EPSP is expected to be larger—cannot be entirely excluded.

The developmental changes reported from P16 to P21 did not affect the induction of LTP in L4: at both ages, LTD was the predominant form of long-term synaptic plasticity and engages either mGluR or NMDAR depending on the pattern of activity used for induction. The transition from P21 to P25 was marked by additional changes in neuronal and synaptic properties. There was a significant decrease in R_{in} and an increase in the NMDAR-dependent component of the EPSP. In addition, there was a sharp change in sign of LTP. Although spike-timing LTD could not be induced, slow-wave presynaptic bursting induced a form of NMDAR-dependent LTP. These data demonstrate that the transition from the precritical to the critical period for visual cortical plasticity is marked by changes in neuronal and synaptic properties that determine a significant shift in synaptic responsiveness to patterns of activity.

Different mechanisms for plasticity in L4

The process of maturation of recurrent excitatory synapses had profound effects on the mechanism involved in the induction and expression of LTP. At P16–P21, only LTD was induced at L4 recurrent synapses independently of the pattern of activity. Despite being induced in the same developmental epoch, spike-timing LTD and slow-wave LTD engaged different glutamatergic receptors and expression mechanisms. Presynaptic and postsynaptic correlated firing activated mGluR-dependent mechanisms for spike-timing LTD (mGluR–LTD). Similar to data reported previously in the barrel cortex (Egger et al., 1999; Bender et al., 2006), our analysis support the interpretation that this form of plasticity was expressed presynaptically. Although our data and analysis point to a presynaptic site of expression for spike-timing LTD, the lack of changes in PPR after induction does not exclude the possibility that additional postsynaptic mechanisms may be involved in the expression of this form of plasticity. During the precritical period, LTD was also induced by slow-wave presynaptic bursting, a paradigm designed to mimic the spontaneous and sparse ongoing activity in developing V1 (Rochefort et al., 2009). However, slow-wave LTD engaged presynaptic NMDARs (NMDAR–LTD). Both forms of LTD involved presynaptic mechanisms of expression, but spike-timing LTD did not show any change in PPR after induction, whereas slow-wave LTD induced a marked reduction in PPR likely attributable to a progressive decrease in neurotransmitter release in response to subsequent action potentials in a train. The progressive increase in depression together with the decrease in PPR suggest that additional presynaptic mechanisms, such as depletion of synaptic resources or refractoriness of release machinery, may be involved in addition to changes in the probability of release. A possible interpretation of these findings is that spike-timing LTD and slow-wave LTD may affect neurotransmitter release through different mechanisms. The involvement of additional postsynaptic mechanisms of expression, such as silencing or loss of functional postsynaptic sites, in the expression of both forms of plasticity cannot be excluded.

What is the role of mGluR–LTD and NMDAR–LTD in visual cortical development? Recent theoretical work suggests that

mGluR–LTD may be involved in the initial stages of the formation of receptive fields (Tanaka and Miyashita, 2009), suggesting a fundamental role for this form plasticity in the early development of visual function. Alterations of mGluR–LTD in the hippocampus have also been associated with neurodevelopmental disorders (Auerbach and Bear, 2010), supporting the possibility that this form of plasticity may be crucial for proper wiring of neural circuits early in development. NMDAR–LTD may be involved in different aspects of visual cortical development. Previously published work showed that NMDAR activity is important for the development of orientation selectivity during early postnatal development (Fagiolini et al., 2003). NMDAR–LTD in the precritical period may thus be a candidate synaptic mechanism for the refinement of orientation preference.

During the critical period, correlated presynaptic and postsynaptic firing failed to change the strength of recurrent excitatory synapses in L4. However, slow-wave presynaptic bursting induced an NMDAR-dependent form of LTP that was expressed presynaptically (NMDAR–LTP). Thus, the same induction paradigm, slow-wave presynaptic bursting, engaged NMDARs in LTD or LTP depending on the state of maturation of L4 recurrent excitatory synapses. A possible explanation for this may rely on the different contribution of NMDARs to the EPSP. Both slow-wave LTP and slow-wave LTD are mediated by presynaptic NMDARs. However, APV has a significant effect on the amplitudes of baseline EPSPs elicited by presynaptic action potentials only at the later age. The reduction in EPSP amplitude after APV bath application at P25–P28 may come from a developmentally regulated change in the contribution of presynaptic NMDAR to action potential-evoked neurotransmitter release during the critical period.

When our entire dataset is interpreted in the context of previous findings, some interesting differences emerge. The requirements for plasticity at recurrent excitatory synapses in L4 differed from those shown for feedforward synapses from L4 onto L2/3 and from recurrent synapses in L5 on a number of accounts. Different from a previous studies (Sjöström et al., 2003; Bender et al., 2006; Corlew et al., 2007; Rodríguez-Moreno and Paulsen, 2008) there is no evidence for NMDAR involvement in the form of spike-timing LTD we report. However, spike-timing LTD at recurrent L4 synapses requires mGluRs similar to that induced at the same synapses in the barrel cortex (Egger et al., 1999). Presynaptic NMDARs are involved in the induction of precritical period slow-wave LTD and critical period slow-wave LTP. Together with previous findings on the developmental regulation of presynaptic NMDAR at glutamatergic synapses in V1 (Corlew et al., 2007), our data suggest that these receptors may still be present well into the critical period but be localized on presynaptic terminals of recurrent L4 synapses between pyramidal neurons. In addition, whereas all previous reports indicated that presynaptic NMDAR are involved in LTD induction only (Sjöström et al., 2003; Bender et al., 2006; Corlew et al., 2007; Rodríguez-Moreno and Paulsen, 2008), our data show that these receptors can contribute to LTP as well but in a developmentally regulated manner.

Visual experience and excitatory synaptic plasticity

The critical period is a time in postnatal development in which sensory experience plays a fundamental role in the proper wiring of cortical circuits (Hubel and Wiesel, 1970). Forms of synaptic plasticity specific for this time window are thought to be the mechanisms driving the experience-dependent refinement of the visual cortical circuit (Kirkwood et al., 1996; Maffei et al., 2006, 2010; Yazaki-Sugiyama et al., 2009; Yoon et al., 2009).

Our data show that visual experience early during postnatal development is necessary for the engagement of cellular mechanisms for induction and expression of LTP during the critical period. Reduced visual input by MD did not affect baseline EPSP amplitude and short-term dynamics of synaptic responses demonstrating that the absence of visual drive does not actively change the strength of recurrent synapses in L4. In addition, MD did not affect intrinsic properties of pyramidal neurons in L4, indicating that brief reduction in visual drive does not modify the excitability and the connectivity of the pyramidal neurons. Previously published work indicates that MD lowers the activation of L4 pyramidal neurons driven by the deprived eye by increasing inhibition onto L4 neurons (Maffei et al., 2006). Increased inhibition may prevent pyramidal neurons from depolarizing sufficiently to fire bursts of action potentials during slow-wave activity, thus impairing LTP induction while leaving baseline excitatory synaptic properties unaffected. Our data indicate that visual experience is permissive for the induction of slow-wave LTP. This interpretation is based on the finding that brief MD not only impaired slow-wave LTP induction, but shifted the sign of recurrent excitatory plasticity to LTD. The MD-dependent switch from LTP to LTD is specific to the critical period, because previous data reported that MD during the precritical period potentiates recurrent excitatory synapses possibly by inducing of a form of homeostatic plasticity (Maffei et al., 2004).

What is driving the shift in sign of plasticity? In our experiments, MD was started after the opening of the critical period; thus, it is unlikely that the switch from slow-wave LTP to LTD after MD depends on impaired maturation of recurrent excitatory synapses. In favor of this interpretation, the form of LTD induced in slices from the deprived hemisphere does not engage the same mechanisms of expression of slow-wave LTD because it is not accompanied by changes in PPR and short-term plasticity. Based on extant literature, one may speculate on a few possible explanations for the experience-dependent switch in sign of excitatory plasticity. Experience-dependent changes in the level of neuromodulators (Seol et al., 2007), changes in the level of neurotrophic factors (Sermasi et al., 2000; Abidin et al., 2006), or changes in L4 pyramidal neurons attributable to potential interactions with other elements of the visual cortical circuit and their plasticity (Maffei et al., 2006) may affect the engagement of synaptic and cellular mechanisms necessary for induction and expression of slow-wave LTP. Alternatively, MD may induce forms of metaplasticity (Abraham and Bear, 1996; Cho and Bear, 2010) that lead to the flip in the sign of activity-dependent plasticity.

References

Abidin I, Köhler T, Weiler E, Zoidl G, Eysel UT, Lessmann V, Mittmann T (2006) Reduced presynaptic efficiency of excitatory synaptic transmission impairs LTP in the visual cortex of BDNF-heterozygous mice. Eur J Neurosci 24:3519–3531.

Abraham WC, Bear MF (1996) Metaplasticity: the plasticity of synaptic plasticity. Trends Neurosci 19:126–130.

Auerbach BD, Bear MF (2010) Loss of the fragile X mental retardation protein decouples metabotropic glutamate receptor dependent priming of long-term potentiation from protein synthesis. J Neurophysiol 104:1047–1051.

Bekkers JM, Stevens CF (1990) Presynaptic mechanism for long-term potentiation in the hippocampus. Nature 346:724–729.

Bélanger MC, Di Cristo G (2011) Sensory experience differentially modulates the mRNA expression of the polysialyltransferases ST8SiaII and ST8SiaIV in postnatal mouse visual cortex. PLoS One 6:e24874.

Bender VA, Bender KJ, Brasier DJ, Feldman DE (2006) Two coincidence

detectors for spike timing-dependent plasticity in somatosensory cortex. J Neurosci 26:4166–4177.
Castelo-Branco M, Neuenschwander S, Singer W (1998) Synchronization of visual responses between the cortex, lateral geniculate nucleus, and retina in the anesthetized cat. J Neurosci 18:6395–6410.
Chen L, Cooper NG, Mower GD (2000) Developmental changes in the expression of NMDA receptor subunits (NR1, NR2A, NR2B) in the cat visual cortex and the effects of dark rearing. Brain Res Mol Brain Res 78:196–200.
Cho KK, Bear MF (2010) Promoting neurological recovery of function via metaplasticity. Future Neurol 5:21–26.
Corlew R, Wang Y, Ghermazien H, Erisir A, Philpot BD (2007) Developmental switch in the contribution of presynaptic and postsynaptic NMDA receptors to long-term depression. J Neurosci 27:9835–9845.
Crozier RA, Wang Y, Liu CH, Bear MF (2007) Deprivation-induced synaptic depression by distinct mechanisms in different layers of mouse visual cortex. Proc Natl Acad Sci U S A 104:1383–1388.
Daw N, Rao Y, Wang XF, Fischer Q, Yang Y (2004) LTP and LTD vary with layer in rodent visual cortex. Vis Res 44:3377–3380.
Desai NS, Cudmore RH, Nelson SB, Turrigiano GG (2002) Critical periods for experience-dependent synaptic scaling in visual cortex. Nat Neurosci 5:783–789.
Di Cristo G, Chattopadhyaya B, Kuhlman SJ, Fu Y, Bélanger MC, Wu CZ, Rutishauser U, Maffei L, Huang ZJ (2007) Activity-dependent PSA expression regulates inhibitory maturation and onset of critical period plasticity. Nat Neurosci 10:1569–1577.
Egger V, Feldmeyer D, Sakmann B (1999) Coincidence detection and changes of synaptic efficacy in spiny stellate neurons in rat barrel cortex. Nat Neurosci 2:1098–1105.
Erisir A, Harris JL (2003) Decline of the critical period of visual plasticity is concurrent with the reduction of NR2B subunit of the synaptic NMDA receptor in layer 4. J Neurosci 23:5208–5218.
Fagiolini M, Pizzorusso T, Berardi N, Domenici L, Maffei L (1994) Functional postnatal development of the rat primary visual cortex and the role of visual experience: dark rearing and monocular deprivation. Vis Res 34:709–720.
Fagiolini M, Katagiri H, Miyamoto H, Mori H, Grant SG, Mishina M, Hensch TK (2003) Separable features of visual cortical plasticity revealed by *N*-methyl-D-aspartate receptor 2A signaling. Proc Natl Acad Sci U S A 100:2854–2859.
Farley BJ, Yu H, Jin DZ, Sur M (2007) Alteration of visual input results in a coordinated reorganization of multiple visual cortex maps. J Neurosci 27:10299–10310.
Feller MB, Scanziani M (2005) A precritical period for plasticity in visual cortex. Curr Opin Neurobiol 15:94–100.
Frenkel MY, Bear MF (2004) How monocular deprivation shifts ocular dominance in visual cortex of young mice. Neuron 44:917–923.
Hensch TK (2004) Critical period regulation. Annu Rev Neurosci 27:549–579.
Hubel DH, Wiesel TN (1970) The period of susceptibility to the physiological effects of unilateral eye closure in kittens. J Physiol 206:419–436.
Jiang B, Treviño M, Kirkwood A (2007) Sequential development of long-term potentiation and depression in different layers of the mouse visual cortex. J Neurosci 27:9648–9652.
Katagiri H, Fagiolini M, Hensch TK (2007) Optimization of somatic inhibition at critical period onset in mouse visual cortex. Neuron 53:805–812.
Kirkwood A, Rioult MC, Bear MF (1996) Experience-dependent modification of synaptic plasticity in visual cortex. Nature 381:526–528.
Li Y, Fitzpatrick D, White LE (2006) The development of direction selectivity in ferret visual cortex requires early visual experience. Nat Neurosci 9:676–681.
Maffei A, Turrigiano G (2008a) The age of plasticity: developmental regulation of synaptic palsticity in neocortical microcircuits. Prog Brain Res 169:211–223.
Maffei A, Turrigiano GG (2008b) Multiple modes of network homeostasis in visual cortical layer 2/3. J Neurosci 28:4377–4384.
Maffei A, Nelson SB, Turrigiano GG (2004) Selective reconfiguration of layer 4 visual cortical circuitry by visual deprivation. Nat Neurosci 7:1353–1359.
Maffei A, Nataraj K, Nelson SB, Turrigiano GG (2006) Potentiation of cortical inhibition by visual deprivation. Nature 443:81–84.
Maffei A, Lambo ME, Turrigiano GG (2010) Critical period for inhibitory plasticity in rodent binocular V1. J Neurosci 30:3304–3309.
Majewska A, Sur M (2003) Motility of dendritic spines in visual cortex in vivo: changes during the critical period and effects of visual deprivation. Proc Natl Acad Sci U S A 100:16024–16029.
Malinow R, Tsien RW (1990) Presynaptic enhancement shown by whole-cell recordings of long-term potentiation in hippocampal slices. Nature 346:177–180.
McGee AW, Yang Y, Fischer QS, Daw NW, Strittmatter SM (2005) Experience-driven plasticity of visual cortex limited by myelin and Nogo receptor. Science 309:2222–2226.
Mellios N, Sugihara H, Castro J, Banerjee A, Le C, Kumar A, Crawford B, Strathmann J, Tropea D, Levine SS, Edbauer D, Sur M (2011) miR-132, an experience-dependent microRNA, is essential for visual cortex plasticity. Nat Neurosci 14:1240–1242.
Nataraj K, Le Roux N, Nahmani M, Lefort S, Turrigiano G (2010) Visual deprivation suppresses L5 pyramidal neuron excitability by preventing the induction of intrinsic plasticity. Neuron 68:750–762.
Quinlan EM, Philpot BD, Huganir RL, Bear MF (1999) Rapid, experience-dependent expression of synaptic NMDA receptors in visual cortex in vivo. Nat Neurosci 2:352–357.
Rao Y, Daw NW (2004) Layer variations of long-term depression in rat visual cortex. J Neurophysiol 92:2652–2658.
Roberts EB, Ramoa AS (1999) Enhanced NR2A subunit expression and decreased NMDA receptor decay time at the onset of ocular dominance plasticity in the ferret. J Neurophysiol 81:2587–2591.
Rochefort N, Garaschuk O, Milos R, Narushima M, Marandi N, Pichler B, Kovalchuk Y, Konnerth A (2009) Sparsification of neuronal activity in the visual cortex at eye-opening. Proc Natl Acad Sci U S A 106:15049–15054.
Rodríguez-Moreno A, Paulsen O (2008) Spike timing-dependent long term depression requires presynaptic NMDA receptors. Nat Neurosci 11:744–745.
Seol GH, Ziburkus J, Huang S, Song L, Kim IT, Takamiya K, Huganir RL, Lee HK, Kirkwood A (2007) Neuromodulators control the polarity of spike-timing-dependent synaptic plasticity. Neuron 55:919–929.
Sermasi E, Margotti E, Cattaneo A, Domenici L (2000) Trk B signalling controls LTP but not LTD expression in the developing rat visual cortex. Eur J Neurosci 12:1411–1419.
Sjöström PJ, Turrigiano GG, Nelson SB (2003) Neocortical LTD via coincident activation of presynaptic NMDA and cannabinoid receptors. Neuron 39:641–654.
Sola E, Prestori F, Rossi P, Taglietti V, D'Angelo E (2004) Increased neurotransmitter release during long-term potentiation at mossy fibre-granule cell synapses in rat cerebellum. J Physiol 557:843–861.
Tagawa Y, Kanold PO, Majdan M, Shatz CJ (2005) Multiple periods of functional ocular dominance plasticity in mouse visual cortex. Nat Neurosci 8:380–388.
Tanaka S, Miyashita M (2009) Constraint on the number of synaptic inputs to a visual cortical neuron controls receptive field formation. Neural Comput 21:2554–2580.
Tanaka S, Tani T, Ribot J, O'Hashi K, Imamura K (2009) A postnatal critical period for orientation plasticity in the cat visual cortex. PLoS One 4:e5380.
Trachtenberg JT, Trepel C, Stryker MP (2000) Rapid extragranular plasticity in the absence of thalamocortical plasticity in the developing primary visual cortex. Science 287:2029–2032.
Wallace W, Bear MF (2004) A morphological correlate of synaptic scaling in visual cortex. J Neurosci 24:6928–6938.
Wang XF, Daw NW (2003) Long term potentiation varies with layer in rat visual cortex. Brain Res 989:26–34.
Weliky M (2000) Correlated neuronal activity and visual cortical development. Neuron 27:427–430.
Wernig A (1975) Estimates of statistical release parameters from crayfish and frog neuromuscular junction. J Physiol 244:207–221.
Yazaki-Sugiyama Y, Kang S, Câteau H, Fukai T, Hensch TK (2009) Bidirectional plasticity in fast-spiking GABA circuits by visual experience. Nature 462:218–221.
Yoon BJ, Smith GB, Heynen AJ, Neve RL, Bear MF (2009) Essential role for a long-term depression mechanism in ocular dominance plasticity. Proc Natl Acad Sci U S A 106:9860–9865.